

Enhancing Mechanical and Thermal Properties of Natural Rubber Composites via Nanocellulose Reinforcement from Coconut Shell Waste: A Sustainable Approach

Isha Meshram¹, Tanushree Bhattacharjee², Suchismita Sahoo³

^{1,2}Vishwakarma Institute of Technology, Pune and 411037, India

³Indian Rubber Manufacturing and Research Association, Thane and 400604, India

*Corresponding Author: Isha Meshram, Vishwakarma Institute of Technology, Pune and 411037, India

Abstract

In recent years, there has been significant interest in the development of nanocellulose and nanocellulose-reinforced composites due to their remarkable properties. This study explores the potential of utilizing coconut shell powder, a renewable and sustainable agricultural byproduct, as a filler in natural rubber composites. Coconut shells, which are often considered waste, offer distinct advantages, including high mechanical strength, light weight, and low cost. In this research, nanocellulose was extracted from coconut shell powder through acid hydrolysis and incorporated into a natural rubber matrix. The mechanical and thermal performance of the resulting composites was evaluated using a Monsanto Rheometer to determine processing parameters and curing behavior. Key mechanical properties, such as tensile strength, tear strength, and hardness, were measured, while swelling studies assessed crosslink density and the reinforcing effect of the filler. Scanning electron microscopy revealed improvements in the composite's morphology, corresponding with enhanced mechanical properties. The results show that nanocellulose derived from coconut shell powder is an effective filler for natural rubber, offering superior physicochemical properties compared to unmodified coconut shell powder. Additionally, the inclusion of this nanocellulose improved the thermal performance of the material, making it a promising candidate for sustainable, high-performance composites.

Keywords: Coconut shell powder Nanocellulose, Natural Rubber, Biowaste, Sustainable materials, Material Characterization.

1. INTRODUCTION

In recent years, the social and environmental impacts associated with fossil fuel extraction have spurred interest in more eco-friendly alternatives. A key focus of recent research has been the utilization of agricultural waste, which consists primarily of three main components: cellulose, hemicellulose, and lignin. Among these, cellulose stands out as a highly abundant renewable resource. It forms through repetitive hydrogen bonding of β -1,4-glycosidic linkages, creating a biological macromolecule with polymorphic characteristics. Natural cellulose exhibits high crystallinity, comprising both crystalline and amorphous regions. Virtually all biomass sources can serve as cellulose providers, including commodity crops like wood and agricultural byproducts, as well as marine algae, bacteria, fungi, and even tunicates.

To produce nanocellulose, the raw material undergoes pretreatment to remove non-cellulosic components such as lignin, hemicellulose, lipids, waxes, pectin, and alginates. Following this, various methods—chemical, physical, and biological—can be employed to extract nanocellulose with diameters ranging from 1 to 100 nm [16].

The acid hydrolysis method remains one of the most effective techniques for producing nanocellulose, though it presents challenges in terms of waste recovery [6]. In contrast, enzymatic hydrolysis is more environmentally friendly but often proves to be less efficient. Consequently, there is a growing interest in developing more effective and eco-conscious processing techniques.

Nanocellulose retains the renewable and biodegradable properties of wood, and its extensive interfacial area allows for a low filler percentage to achieve a significant reinforcing effect. Additionally, the high

density of hydroxyl groups on its surface facilitates easier functionalization. This versatile material finds applications across various fields, including reinforcing fillers, the paper industry, electronics, packaging, biological scaffolds, and pharmaceutical carriers. The use of nanocellulose in reinforced composite materials is particularly notable, with established techniques leading to well-developed end products [17].

Recent findings indicate that nanocellulose derived from coconut shell powder serves as an efficient natural rubber filler at parts per hundred loadings. These composites exhibit superior physicomaterial properties due to the enhanced reinforcing ability of nanocellulose compared to unmodified coconut shell powder. Furthermore, incorporating coconut shell powder into a natural rubber matrix enhances the thermal properties of the material. Advances in nanocellulose modification and a broader selection of matrix materials suggest a promising future for this material [6].

2. THEORETICAL REFERENCE

Nanocellulose, derived from cellulose, has garnered significant attention due to its exceptional properties such as high mechanical strength, lightweight nature, and renewability. Cellulose is predominantly sourced from agricultural byproducts, including coconut shells, which are rich in cellulose and offer a sustainable resource for nanocellulose production (2, 33). The extraction methods for nanocellulose, primarily acid hydrolysis, effectively yield nanostructures with diameters ranging from 1 to 100 nm, although challenges related to waste recovery and efficiency remain (1, 13). Recent advancements have introduced alternative techniques such as steam explosion and ultrasound-assisted extraction, which enhance yield while reducing environmental impacts (9, 12). Incorporating nanocellulose into natural rubber matrices has shown promising results, improving mechanical properties like tensile strength and thermal stability (4, 6, 10). This incorporation capitalizes on the high aspect ratio and extensive surface area of nanocellulose, allowing for effective stress transfer within the composite (25). Furthermore, utilizing agricultural waste for nanocellulose production aligns with sustainability goals and presents economic advantages by reducing reliance on fossil fuels (3, 26). Overall, the development of nanocellulose from coconut shell powder signifies a vital step towards innovative, eco-friendly materials in various industrial applications (5, 11, 21).

3. MATERIALS AND METHODS

Coconut shells were collected from local markets and restaurants as bio-waste. The other reagents used included distilled water, toluene, ethanol, sodium hypochlorite, hydrochloric acid, and potassium hydroxide (KOH). All materials were of analytical grade.

3.1. Isolation of Cellulose

The collected coconut shells were cleaned, the coir was removed, and the shells were dried in an oven for 3–4 hours. The dried shells were then crushed and pulverized into a fine powder. The powder, sieved through a 200-mesh filter, was washed with distilled water for 1 hour under continuous stirring, followed by straining. It was further washed with ethanol for 30 minutes under stirring and strained again. The powder was placed in an oven at 80°C for 1 hour.

Dewaxing was performed using a Soxhlet apparatus with a 2:1 mixture of toluene/ethanol for 6 hours. Afterward, the powder was bleached using 0.7% (w/v) sodium hypochlorite at 75°C for 1 hour to remove lignin. This bleaching process was repeated six times. The residue was washed with distilled water until it reached a neutral pH.

To remove hemicellulose, the sample was treated with 2% KOH at 90°C for 2 hours under constant stirring at 45°C. The resulting residue was washed until a neutral pH was obtained, and then dried at room temperature.

3.2. Preparation of Nanocellulose

The isolated cellulose was hydrolyzed using hydrochloric acid (HCl) in a cellulose-to-HCl ratio of 1:25. Various conditions, including HCl concentration, temperature, and hydrolysis time, were tested. The resulting colloidal suspension was sonicated for 10 minutes to homogenize the nanocellulose. The residue was strained after 1 hour, and the process was repeated six times. To achieve a neutral pH, the residue was rinsed with distilled water, and a strong base was added. To ensure hemicellulose removal,

the sample was treated with 2% KOH at 90°C for 2 hours under steady stirring at 45°C. The sample was again washed to neutral pH and dried at room temperature.

3.3. Infrared Spectroscopy (IR) Analysis

The FTIR analysis of coconut shell powder highlights the successful removal of lignin and hemicellulose during the isolation of cellulose. The spectrum shows a prominent O-H stretching vibration at 3350 cm^{-1} , indicating the presence of hydroxyl groups in the cellulose structure. The C-H stretching vibration at 2920 cm^{-1} confirms the presence of alkane groups, which are typical in cellulose. The peak around 1730 cm^{-1} corresponds to the C=O stretching vibration, which suggests the presence of carboxylic groups, likely from residual hemicellulose or lignin. Additionally, peaks at 1507 cm^{-1} and 1240 cm^{-1} , which are attributed to lignin, confirm that lignin was initially present but was effectively removed during the treatment process. The peak at 1033 cm^{-1} , representing the C-O-C stretching vibration in the pyranose ring, is characteristic of cellulose, confirming its successful isolation. Overall, the FTIR results validate the removal of unwanted components and the presence of pure cellulose after the treatment.

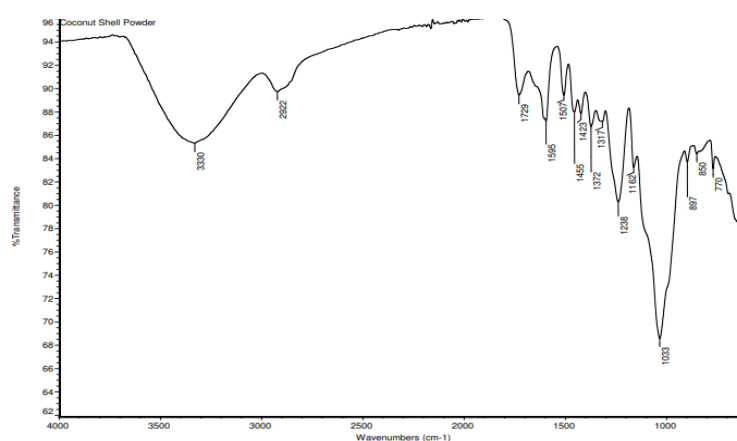


Figure 1. Graph of FTIR spectra of Coconut Shell Powder Nanocellulose

4. SCANNING ELECTRON MICROSCOPY (SEM) ANALYSIS

The SEM images provide clear evidence of the morphological changes that occurred during the isolation of nanocellulose from coconut shell powder. In the initial stages (Figure 2, magnification 615X), the raw coconut shell powder exhibited irregularly shaped, large agglomerates. However, after the chemical treatments, the SEM images (Figure 2, magnification 273X) reveal a significant reduction in particle size. The images show the presence of nanofibrils with diameters ranging from 5 to 20 nm, indicating the successful breakdown of cellulose into its nanoscale components. Additionally, spherical nanostructures were observed after sonication, suggesting the formation of cellulose nanospheres due to the inherent hydrophilicity of cellulose, which may have led to some agglomeration. Residual amorphous cellulose was also visible, contributing to the morphology observed in the images. The SEM analysis confirms the successful transformation of the coconut shell powder into nanocellulose with nanoscale fibrils and spheres, suitable for various applications in nanotechnology and materials science.

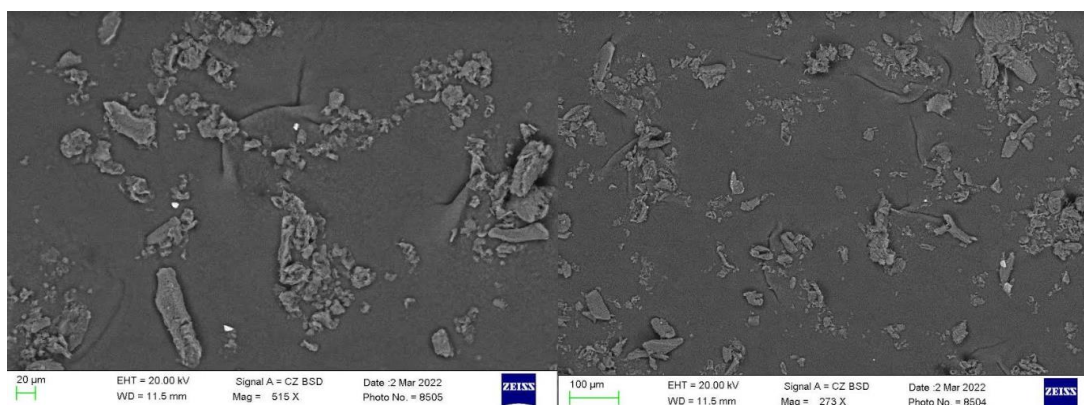


Figure 2. SEM of Coconut Shell Powder Nanocellulose

5. RUBBER COMPOUND

5.1. Preparation of Sample

Table 1 shows the formulation. All elements were mixed using a Brabender mixer and typical laboratory two roll mill (160*300mm) by ASTM D3184-80. All composites had the same nip gap, mill roll speed ratio, mixing duration, and component addition sequence. For 24 hours, the sheeted compound was conditioned at room temperature. Table 1 shows the formulation. All elements were mixed using a Brabender mixer typical laboratory two roll mill (160*300mm) under ASTM D3184-80. All composites had the same nip gap, mill roll speed ratio, mixing duration, and component addition sequence. For 24 hours, the sheeted compound was conditioned at room temperature [27].

Table 1. Compound formulation (all ingredients are parts per hundred gram of rubber phr)

Material	Control	NR+NC	NR+NC
Natural Rubber	100	100	100
Nanocellulose	-	5	10
Zinc Oxide	3	3	3
Stearic Acid	1	1	1
6PPD	1	1	1
Sulphur	2	2	2
MBTS--2-2'-Dithiobis(benzothiazole)	1.5	1.5	1.5

5.2. Rheological Properties

The rheological properties of rubber compounds, including cure characteristics, were assessed using a Monsanto Moving Die Rheometer (MDR 2000) at 160°C for 1 hour, with an oscillating angle of 0.35°, according to ASTM D5289. The results, presented in Table 2, show the curing behavior of natural rubber (NR) and NR mixed with 5 phr and 10 phr of nanocellulose derived from coconut shells. The inclusion of nanocellulose increases the fluidity of the rubber compound. This is evidenced by the increase in torque values with higher nanocellulose loadings, which indicates that as more filler is dispersed into the rubber matrix, the mobility of the rubber's macromolecular chains decreases, leading to stiffer vulcanizates [37].

The optimal cure time, minimum torque (ML), maximum torque (MH), and scorch time of the nanocellulose-filled rubber composites are also detailed in Table 2. Despite the increase in filler loading, both the scorch time and the optimal cure time decreased, suggesting that as filler loading increases, the filler integrates more quickly into the rubber matrix, generating greater resistance and heat during curing. This results in a faster curing process. The data suggest that the addition of nanocellulose to natural rubber composites not only enhances the stiffness but also affects the curing dynamics by decreasing the time required for full crosslinking to occur.

Table 2. Cure Characteristics of Rubber Compounds

Sample	Temp (°C)	ML (Lbin)	MH (Lbin)	Scorch time (TS 1)	Scorch time (TS 2)	t90
Natural rubber	160	0.83	4.32	3.04	3.86	5.19
Natural Rubber ++5phr Nanocellulose	160	0.44	2.97	3.96	6.49	6.09
Natural Rubber ++10phr Nanocellulose	160	0.68	10.01	9.66	10.09	9.59

5.3. Curing Process of Rubber Compound

The curing process of the rubber compound was carried out in accordance with ASTM D3182 standards using an electrically heated hydraulic press from M/S Hind Hydraulics, New Delhi, India. Compression molding was performed at 160°C under a pressure of 3000 psi, with the cure time set at t90 plus an additional 2 minutes for tensile specimen preparation. Following vulcanization, the samples were conditioned for 24 hours at room temperature before being subjected to further testing and analysis.

5.4. Physical Testing and Characterization

5.4.1. Tensile Properties, Hardness, and Aging of Samples

Tensile properties were evaluated according to ASTM standards, which included measurements of tensile strength (kg/cm²), elongation at break (%), and modulus at varying strain levels (kg/cm²). These

tests were conducted on Type C tensile dumbbells, which were die-cut from molded rubber sheets using a hollow die punch. The hardness of each sample was determined using a Shore A hardness meter in accordance with ASTM D2240. An average of five measurements was recorded for each sample. The tensile test specimens were subjected to air aging in a controlled environment at 100°C for 72 hours. For crosslink density testing, the vulcanized rubber samples were cut into smaller pieces (1 cm × 1 cm with a thickness of 3–5 mm). Crosslink density testing was performed using a multi-cell aging oven provided by M/s Tempo Industries, as per ASTM D6814-02 guidelines [20].

5.4.2. FTIR/ATR, Crosslink Density, and Scanning Electron Microscopy (SEM)

Fourier Transform Infrared Spectroscopy (FTIR) in Attenuated Total Reflectance (ATR) mode was employed to quickly acquire the infrared spectrum of the rubber samples. The ATR method involved pressing the rubber sample against a prism to obtain the spectral data, allowing for the analysis of chemical structures. Crosslink density was measured to investigate the molecular network of the rubber, in accordance with ASTM D6814-02 standards. The dispersion of fillers, particularly nanocellulose, within the rubber matrix was studied using Scanning Electron Microscopy (SEM). The SEM analysis was performed on a JSM 5600 LV microscope (JEOL, Tokyo, Japan) at a magnification of 100x. The fractured surface of the rubber samples was examined to assess the distribution and interaction of the fillers within the rubber matrix [25].

5.4.3. Differential Scanning Calorimetry (DSC) and Thermogravimetric Analysis (TGA)

The glass transition temperature (T_g) of all vulcanized rubber samples was determined using a Differential Scanning Calorimeter (DSC) (PerkinElmer 6000). The thermal stability of the vulcanized rubber was assessed using a Thermogravimetric Analyzer (TGA Q50, TA Instruments). The TGA measurements were performed by heating the samples from ambient temperature to 900°C at a heating rate of 20°C/min. These thermal analyses provided insights into the thermal behavior and degradation characteristics of the rubber composites, particularly the influence of nanocellulose as a reinforcing filler [25].

6. RESULTS AND DISCUSSION

6.1. Tensile Strength

The tensile strength of rubber composites reinforced with coconut shell powder was evaluated across varying filler loadings, revealing a maximum strength at 5 phr (parts per hundred rubber). This superior performance at 5 phr can be attributed to the uniform distribution of the filler within the natural rubber (NR) matrix, which enhances the interfacial region and promotes better interaction between the filler and the rubber. The smaller particle size and effective dispersion of the filler contribute significantly to the observed improvement in tensile strength. However, an increase in filler loading to 10 phr results in a noticeable decline in tensile strength. This reduction can be explained by inadequate bonding between the filler particles and the NR matrix, leading to pronounced agglomeration. As the filler content rises, filler-filler interactions dominate, thereby reducing the effective reinforcement that the filler can provide [30].

Table 3 illustrates the tensile properties of rubber composites before aging. It is evident that elongation at break (EB) decreases as filler loading increases. This reduction is expected due to the non-deformable nature of the fillers, which limits the composite's rubber content and results in a dilution effect. Furthermore, the tensile modulus values—M100 (stress at 100% elongation), M200 (stress at 200% elongation), and M300 (stress at 300% elongation)—exhibit slight increases with higher filler content. Since the modulus of the filler powder is considerably greater than that of the NR matrix, it effectively acts as an abrasive particle, enhancing the overall modulus of the composite.

Table 3. Tensile Properties of Rubber Composites before Aging

Sample (Before Ageing)	Thickness (mm)	M100 (MPa)	M200 (MPa)	M300 (MPa)	TS (MPa)	EB (%)
Natural rubber	1.84	0.58	0.77	1.1	11.4	760
Natural Rubber + 5phr Nanocellulose	1.73	0.95	1.2	1.5	15.9	650
Natural Rubber+ 10phr Nanocellulose	1.85	0.69	0.88	1.3	14	800

The aging behavior of the rubber composites, particularly under thermal and oxidative stress, is critical for assessing their long-term performance. Table 4 presents the tensile properties of the composites after

aging. The results indicate that exposure to heat and environmental factors leads to a deterioration in mechanical properties, evidenced by the reduction in tensile strength and elongation at break. The degradation of the molecular structure of NR, exacerbated by the presence of unsaturated C=C bonds, is a key factor in this decline. Additionally, the disruption of filler-rubber bonding due to thermal stress further compromises the mechanical properties.

Table 4. Tensile Properties of Rubber Composites after Aging

Sample(After Ageing)	Thickness (mm)	M100 (MPa)	M200 (MPa)	M300 (MPa)	TS (MPa)	EB (%)
Natural rubber	1.81	0.36	0.65	0.86	10.3	800
Natural Rubber + +5phr Nanocellulose	1.73	0.57	1.26	1.52	14.5	690
Natural Rubber + +10phr Nanocellulose	1.85	0.56	0.86	0.99	13.5	870

The interactions between the polymer and filler play a crucial role in determining the elastic modulus, which is optimized when the filler is uniformly dispersed throughout the polymer matrix. This behavior is influenced by the characteristics of the filler particles and can vary based on the chemical composition of the polymer.

6.2. Hardness

The hardness of the rubber composites was evaluated using the Shore A durometer according to ASTM D-2240 standards. The results indicate that the incorporation of nanocellulose derived from coconut shell powder significantly increases the hardness of each composite, as shown in Table 5. Additionally, aging further enhances the hardness values across all samples.

Aging impacts the mechanical properties of rubber goods, leading to substantial degradation after 72 hours. During the thermos-oxidative process, several free radicals may form in the natural composite material, particularly in unsaturated elastomers, due to exposure to air. These free radicals can subsequently generate hydroxyl peroxides, which react with the elastomer, resulting in the formation of additional alcohol and carboxylic acid groups. Moreover, the effects of elevated temperatures and shear forces following heating can damage the cellulose matrix, contributing to the overall changes in hardness.

Table 5. Hardness Before and after ageing

Sample	Before Ageing Shore A°	After Ageing Shore A°
Natural rubber	35	38
Natural Rubber + 5phr Nanocellulose	33	37
Natural Rubber + 10phr Nanocellulose	40	42

6.3. Crosslinking Density

The swelling ratio in toluene is a critical parameter for estimating the crosslink density of rubber composites. It is defined by the equation:

$$R = \frac{W_s}{W_d} \quad (1)$$

Where W_s is the weight of the swollen sample and W_d is the weight of the desiccated sample after 24 hours. The Flory-Rehner equation can be employed to calculate the crosslink density (ν) of the polymer network, represented as:

$$\nu = \frac{-\ln(1 - V_r)}{X \cdot V_s} \quad (2)$$

In this equation, V_r is the predicted volume fraction of polymer in the swollen mass, X is the polymer-solvent interaction factor, and V_s is the molar volume of the solvent [24].

Additional calculations include the weight of the swollen sample, given by:

$$W_{sol} = W_s - W_d \quad (3)$$

The interaction parameter can be expressed as:

$$X = \frac{\beta \cdot V_s \cdot R \cdot T \cdot ds}{dp} \quad (4)$$

In this context, β represents the lattice parameter (0.38), V_s denotes the solvent's molar volume, R is the universal gas constant, T is the absolute temperature (300 K), d_s is the solvent's solubility factor, and d_p indicates the polymer's solubility factor (where d_s for toluene is 8.9 and d_p for natural rubber (NR) is 8.1). Previous research has established a correlation factor of 0.393 for NR and toluene, which closely aligns with the experimental value of 0.4. The solvent's molar volume and density were calculated to be $V_s=106.2$ mL/mol and $d_s=0.87$ g/cm³, respectively. The swelling ratio, along with the quantity of elastically active chains per unit volume, is utilized to estimate crosslink density. As filler content increases, the swelling ratio decreases, while the quantity of elastically active chains per unit volume increases. These findings indicate that higher filler loading corresponds to a systematic increase in the crosslink density of elastically active chains, thereby enhancing the mechanical properties of the composites. Specifically, the incorporation of limestone dust as a filler in NR composites has demonstrated an increase in polymer strength from 5 to 10 phr filler content, reinforcing previous findings that highlight the importance of specific surface area and filler reinforcing capability in determining the crosslink density of rubber vulcanizates [40, 30].

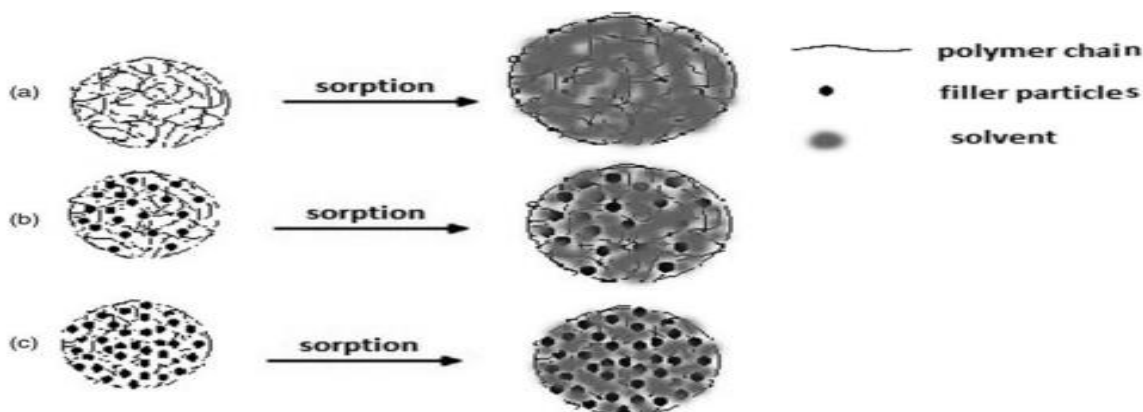


Figure 3. Swelling Behavior of Natural Rubber and Nanocellulose Composites under Toluene Exposure

Figure 3 illustrates the swelling behavior of both natural rubber and nanocellulose composites, revealing that increased filler loading leads to a higher degree of crosslinking. The concentrated hydroxyl functional groups in cellulose facilitate strong filler-filler interactions through hydrogen bonding, creating a coherent gel structure that limits the vulcanization of the rubber matrix and ultimately affects crosslink density.

6.4. Thermogravimetry

The thermogravimetric analysis (TGA) and derivative thermogravimetry (DTG) curves for a 5 phr Natural Rubber-Nanocellulose composite, utilizing Coconut Shell Powder as the filler, provide critical insights into the thermal degradation characteristics and material composition [3]. The first stage of degradation begins at around 50 °C and extends to 300 °C, where the sample experiences a mass loss of 5.89%, which corresponds to the evaporation of moisture and the breakdown of low boiling volatile components. This stage primarily represents the loss of lightweight substances that vaporize at lower temperatures.

As the temperature increases to the range of 300 to 600°C, a substantial mass loss of 88.98% occurs, indicating the decomposition of the polymer matrix, including the natural rubber. This is the principal degradation phase, where the polymer's molecular chains break down and volatiles are released. During this phase, both non-rubber materials and rubber materials degrade. The derivative thermogravimetric (DTG) curve exhibits a sharp peak at approximately 386.77°C, signifying the temperature at which the highest rate of mass loss occurs. This peak is crucial as it represents the point of maximum thermal degradation, which is typical of rubber materials undergoing breakdown.

After 600°C, a smaller mass loss of 2.64% is recorded, which is attributed to the remaining combustible organic materials. Beyond this point, the TGA curve levels off, indicating the thermally stable phase of the material. At temperatures beyond 600°C and up to 860°C, no significant mass loss is observed, and the residual mass, accounting for 2.56%, represents the ash content. This ash is primarily composed of inorganic residues, highlighting the material's thermal stability beyond the primary degradation stages.

The analysis suggests that the incorporation of nanocellulose derived from Coconut Shell Powder, with a particle size of approximately 8 nm, significantly enhances the thermal properties of the natural rubber matrix. The presence of this nanocellulose as a reinforcing filler contributes to increased char residue, implying improved thermal stability and mechanical strength. The nanoscale filler interacts with the polymer matrix, restricting chain mobility and delaying the degradation process. As a result, the composite's mechanical and thermal performance is enhanced, showcasing the beneficial effects of nanoscale reinforcement.

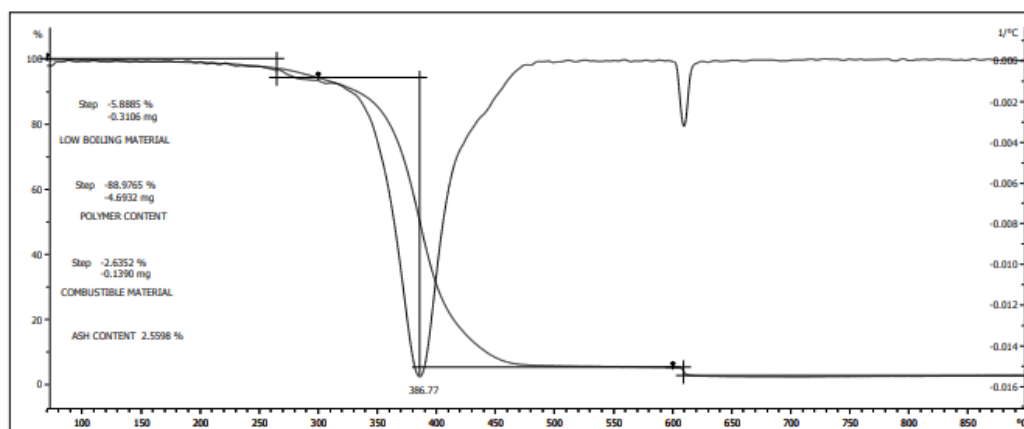


Figure 4. Thermogravimetric Analysis (TGA) of Natural Rubber Composite with 5 phr Nanocellulose from

6.5. Differential Scanning Calorimetry (DSC)

The provided Differential Scanning Calorimetry (DSC) curve illustrates the glass transition behavior of a Natural Rubber composite containing 5 phr nanocellulose derived from Coconut Shell Powder. The glass transition temperature (T_g) is a critical thermal property of polymers, marking the transition from a hard, brittle state to a softer, more flexible state. In this analysis, the onset of the glass transition occurs at $-62.15\text{ }^\circ\text{C}$, while the midpoint, according to ISO standards, is at $-59.76\text{ }^\circ\text{C}$. Below this temperature range, the composite is in a glassy state, where the polymer chains are rigid, leading to a brittle material. As the temperature rises above T_g , the material transitions into a rubbery, flexible state, which is key to its mechanical performance in applications requiring elasticity. The curve shows a noticeable change in heat flow as the material undergoes this phase transition, reflecting the increased molecular mobility in the polymer matrix. This thermal behavior suggests that the composite will maintain its flexibility even at low temperatures, a desirable property for applications such as automotive parts or materials exposed to cold environments. The incorporation of nanocellulose may have influenced this glass transition, possibly enhancing the material's overall performance by improving its mechanical and thermal stability without significantly altering the fundamental properties of the natural rubber.

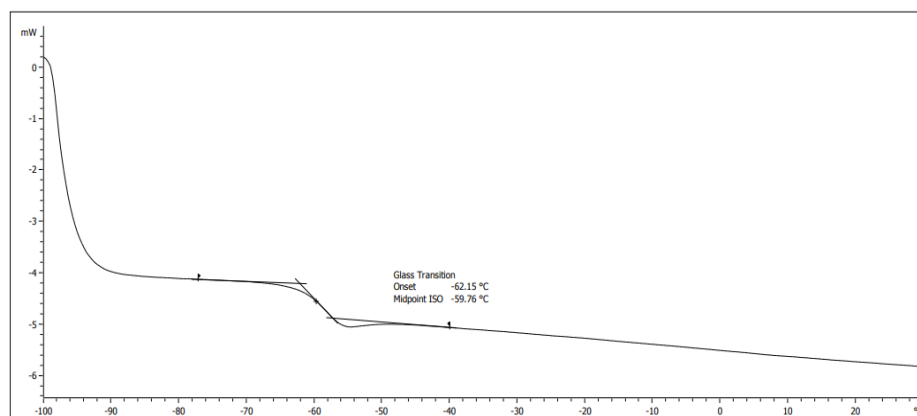


Figure 5. DSC of Natural Rubber Composite with 5 phr Nanocellulose from Coconut Shell Powder.

6.6. X-Ray Diffraction (XRD)

X-ray Diffraction (XRD) is used to determine the crystallinity index of natural rubber and nanocellulose. The crystallinity factor of cellulose and nanocellulose is calculated using peaks at $2\theta =$

20.1° (I200) and $2\theta = 16.3^\circ$ (Iam). Higher acid concentration during hydrolysis affects the crystalline regions, initially increasing the crystallinity index by breaking down the amorphous regions, but excessive acid can also damage the crystalline areas, reducing the crystallinity index. Additionally, the Energy Dispersive X-ray Spectroscopy (EDS) spectrum reveals the elemental composition of the natural rubber-nanocellulose composite, showing significant peaks for oxygen (O), zinc (Zn), and sulfur (S). The high oxygen content indicates the presence of zinc oxide (ZnO), which enhances the mechanical properties and acts as a curing agent in rubber. Sulfur, essential for the vulcanization process, forms cross-links in the rubber, improving its strength and elasticity. Zinc peaks confirm the role of ZnO in reinforcing the composite, contributing to its overall performance and durability. Together, XRD and EDS analyses provide crucial insights into both the structural and compositional properties of the composite [35].

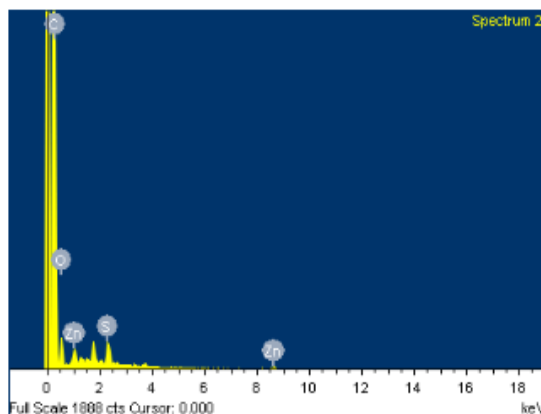


Figure 6. X-ray Diffraction (XRD) of Natural Rubber Composite with 5 phr Nanocellulose from Coconut Shell Powder

6.7. Scanning Electron Microscopy (SEM)

The SEM image of nanocellulose-filled natural rubber, captured at 2000x magnification, highlights an uneven surface with ridges and depressions, suggesting that surface roughness plays a key role in the material's mechanical behavior. The irregular protrusions and scattered particles indicate potential defects, such as impurities or voids, which could weaken the material by acting as stress concentration points. The use of backscattered electron (BSD) imaging enhances contrast, revealing compositional differences and highlighting areas with varying atomic numbers. In the natural rubber vulcanizates with 5 phr nanocellulose, the filler is well-dispersed, significantly reinforcing the matrix and improving mechanical properties like tensile strength and elasticity. However, at higher filler concentrations, poor dispersion and nanocellulose aggregation are evident, which diminish the composite's reinforcing ability. These observations emphasize the importance of achieving optimal nanocellulose dispersion to maximize the mechanical performance and durability of the natural rubber composites. The results suggest that while lower phr loadings exhibit good dispersion and enhanced reinforcement, higher loadings lead to particle aggregation, which undermines the material's properties.

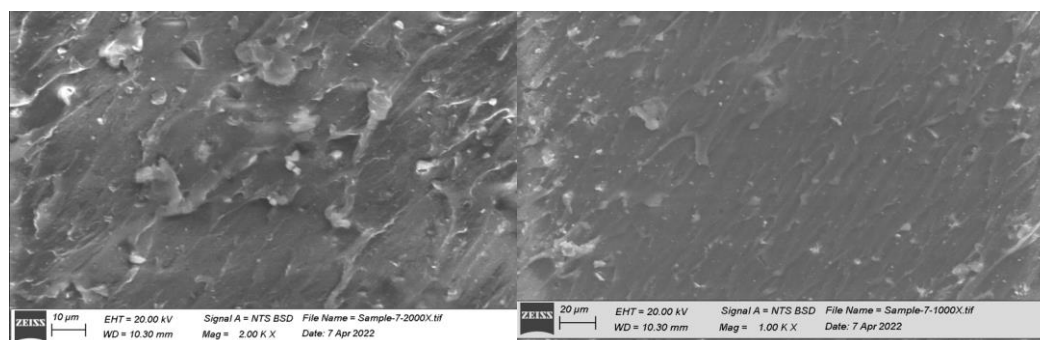


Figure 7. Scanning Electron Microscopy (SEM) Of Natural Rubber Composite With 5 Phr Nanocellulose From Coconut Shell Powder.

7. CONCLUSION

This research highlights the promising application of nanocellulose derived from coconut shell powder as a sustainable alternative to traditional carbon fillers in natural rubber (NR) composites. The optimal

incorporation of 5 phr nanocellulose significantly enhances the mechanical properties of the NR composites, demonstrating superior tensile strength and elasticity. This improvement is attributed to the uniform dispersion of nanocellulose, which fosters effective interfacial bonding and reinforces the rubber matrix, leading to enhanced performance compared to composites filled with conventional carbon materials.

The aging behavior of the composites under thermal and oxidative stress indicates that while all composites experience some degradation, the presence of nanocellulose contributes to improved hardness and thermal stability. The thermogravimetric analysis (TGA) results further substantiate the enhanced thermal performance of the composites, showcasing higher char residue and reduced degradation rates compared to those filled with carbon-based materials. This aspect is crucial for applications requiring durability and longevity.

Differential scanning calorimetry (DSC) analysis revealed that the incorporation of nanocellulose maintains the composite's flexibility at low temperatures, a significant advantage for applications exposed to varying thermal conditions. X-ray diffraction (XRD) and energy dispersive X-ray spectroscopy (EDS) confirmed the structural integrity and beneficial properties imparted by the nanocellulose, reinforcing its role in enhancing mechanical strength without compromising environmental sustainability.

The scanning electron microscopy (SEM) findings illustrate that optimal filler loading at 5 phr achieves effective dispersion and reinforcement, while higher loadings lead to aggregation and reduced mechanical performance. These observations underscore the importance of achieving uniform dispersion to maximize the benefits of nanocellulose in rubber composites.

In summary, this study not only emphasizes the viability of using agricultural waste, such as coconut shells, to produce nanocellulose but also positions nanocellulose as a sustainable and effective alternative to carbon fillers in rubber composites. By replacing conventional carbon fillers with nanocellulose, we can contribute to a more sustainable materials economy, reduce reliance on fossil-derived materials, and promote the circular economy in polymer applications. The findings advocate for further research into the use of nanocellulose in various composite systems, aligning material development with sustainability goals.

ACKNOWLEDGMENTS

The author is thankful to Director Dr. K. Rajkumar, Indian Rubber Manufacturing and Research Association, Thane Mumbai for providing necessary facilities and full support of this research.

REFERENCES

- [1] Alain Dufresne, Nanocellulose: from nature to high performance tailored materials, Walter de Gruyter GmbH 2012.
- [2] Aparna K. Balan, Sreejith Mottakkunnu Parambil, Shaniba Vakyath, Jinitha Thulissery Velayudhan et al. Coconut shell powder reinforced thermoplastic polyurethane/natural rubber blend-composites: effect of silane coupling agents on the mechanical and thermal properties of the composites, *Journal of Materials Science*, 2017.
- [3] C. Sareena, M. T. Ramesan, E. Purushothaman. "Utilization of peanut shell powder as a novel filler in natural rubber", *Journal of Applied Polymer Science*, 2012.
- [4] C. Sareena, M.T. Ramesan, E. Purushothaman. "Transport studies of peanut shell powder reinforced natural rubber composites in aromatic solvents", *Polymer Composites*, 2012.
- [5] Cherian, B.M.; Pothan, L.A.; Nguyen-Chung, T.; Mennig, G.; Kottaisamy, M.; Thomas, S. A novel method for the synthesis of cellulose nanofibril whiskers from banana fibers and characterization. *J. Agric. Food Chem.* 2008, 56, 5617–5627.
- [6] De Rodriguez, N.L.G.; Thielemans, W.; Dufresne, A. Sisal cellulose whiskers reinforced polyvinyl acetate nanocomposites. *Cellulose* 2006, 13, 261–270.
- [7] G. K. Jana, C. K. Das. "Devulcanization of Natural Rubber Vulcanizates by Mechanochemical Process", *Polymer-Plastics Technology and Engineering*, 2005
- [8] H. Ismail, F. S. Haw. "Effects of palm ash loading and maleated natural rubber as a coupling agent on the properties of palm-ash-filled natural rubber composites", *Journal of Applied Polymer Science*, 2008.
- [9] H. Sosiati, D. A. Wijayanti, K. Triyana, B. Kamiel. "Morphology and crystallinity of sisal nanocellulose after

- sonication", AIP Publishing, 2017.
- [10] Haghghat M, Zadhoush A and Khorasani SN. Physicomechanical properties of alpha-cellulose-filled styrene-butadiene rubber composites. *J Appl Polym Sci* 2005;96: 2203–2211.
- [11] Hanafi Ismail, M.R. Edyham, B. Wirjosejono. "Bamboo fibre filled natural rubber composites: the effects of filler loading and bonding agent", *Polymer Testing*, 2002
- [12] Ismail, H.. "Maleated natural rubber as a coupling agent for paper sludge filled natural rubber composites", *Polymer Testing*, 200510.
- [13] Jie Wang, Xin Liu, Tao Jin, Haifeng He, Lei Liu. "Preparation of nanocellulose and its potential in reinforced composites: A review", *Journal of Biomaterial Science, Polymer Edition*, 2019ss.
- [14] Julien B, et al. Mechanical, barrier, and biodegradability properties of bagasse cellulose whiskers reinforced natural rubber nanocomposites. *Ind Crops Prod* 2010; 32:627–633.
- [15] Kentaro Abe, Shinichiro Iwamoto, Hiroyuki Yano. "Obtaining Cellulose Nanofibers with a Uniform Width of 15 nm from Wood", *Biomacromolecules*, 2007.
- [16] Kontturi, E.; Laaksonen, P.; Linder, M.B.; Groschel, A.H.; Rojas, O.J.; Ikkala, O. Advanced Materials through Assembly of Nanocelluloses. *Adv. Mater.* 2018, 30, 39.
- [17] Lua, A.C. "Preparation and characterization of activated carbons from oil-palm stones for gas-phase adsorption", *Colloids and Surfaces A: Physicochemical and Engineering Aspects*, 20010130.
- [18] M Arshad Bashir, M Shahid, Riaz Ahmed, A G Yahya. "Study of rheological, viscoelastic and vulcanization behavior of sponge EPDM/NR blended nano-composites", *IOP Conference Series: Materials Science and Engineering*, 2014.
- [19] M. B. El-Arnaouty, M. Eid, K. S. Atia, A. M. Dessouki. "Characterization and application of grafted polypropylene and polystyrene treated with epichlorohydrin coupled with cellulose or starch for immobilization processes", *Journal of Applied Polymer Science*, 2009.
- [20] Mandal, A.; Chakrabarty, D. Isolation of nanocellulose from waste sugarcane bagasse (SCB) and its characterization. *Carbohydr. Polym.* 2011, 86, 1291–1299. B 2018, 6, 830–843.
- [21] Mohammad Andideh, Ghasem Naderi, Mir Hamid Reza Ghoreishy, Sedigheh Soltani. "Nanocomposites Based on NR/SBR: Effects of Nanoclay and Short Nylon Fibers on the Cure Characteristics and Thermal Properties", *Polymer-Plastics Technology and Engineering*, 2013
- [22] Mohapatra, Sunita, and Golok B. Nando. "Cardanol: a green substitute for aromatic oil as a plasticizer in natural rubber", *RSC Advances*, 2014.
- [23] Moreau, C.; Villares, A.; Capron, I.; Cathala, B. Tuning supramolecular interactions of cellulose nanocrystals to design innovative functional materials. *Ind. Crop. Prod.* 2016, 93, 96–107.
- [24] Munch, A.S.; Wolk, M.; Malanin, M.; Eichhorn, K.J.; Simon, F.; Uhlmann, P. Smart functional polymer coatings for paper with anti-fouling properties. *J. Mat. Chem*
- [25] Nashwan Q. Mahmood, Kálmán Marossy, Peter Baumli. "Effects of nanocrystalline calcium oxide particles on mechanical, thermal, and electrical properties of
- [26] Nunes RCR and Visconte LLY. Natural fibers/elastomeric composites. In: E Frollini, A Leao and LHC Mattoso (eds) *Natural Polymer Agrofiber Based Composites*. Sao Carlos, Brazil, 2000: 135–157.
- [27] Pongdhorn Sae-oui. "Utilization of limestone dust waste as filler in natural rubber", *Journal of Material Cycles and Waste Management*, 2009.
- [28] Qingjun Ding. "Preparation and characterization of composites: EPDM-g-AA/CaCO₃", *Polymer Composites*, 10/2005
- [29] Rattanapan, Apaipan, Jitrakha Paksamut, Pornsri Pakeyangkoon, and Surakit Tuampoemsab. "Waste Silicon Carbide as Filler for Natural Rubber Compounds", *Advanced Materials Research*, 2014.
- [30] S Widiarto, S D Yuwono, A Rochliadi, I M Arcana. "Preparation and Characterization of Cellulose and Nanocellulose from Agro-industrial Waste - Cassava Peel", *IOP Conference Series: Materials Science and Engineering*, 2017
- [31] S. Anandhan, P. P. De, Anil K. Bhowmick, S. K. De, S. Bandyopadhyay. "Thermoplastic elastomeric blend of nitrile rubber and poly(styrene-co-acrylonitrile). II. Replacement of nitrile rubber by its vulcanizate powder", *Journal of Applied Polymer Science*, 2003.
- [32] Salas C, Nypelö T, Abreu C R, Carrillo C and Rojas O J 2014 *Current Opinion in Colloids & Interface Science*. 19 383-396
- [33] Sareena, C., M. Ramesan, and E. Purushothaman. "Utilization of coconut shell powder as a novel filler in natural rubber", *Journal of Reinforced Plastics and Composites*, 2012.
- [34] Shaji Joseph. "Green Composites from Natural Rubber and Oil Palm Fiber: Physical and Mechanical

- Properties", International Journal of Polymeric Materials, 2006.
- [35] Sirvio, J.A.; Visanko, M.; Liimatainen, H. Acidic Deep Eutectic Solvents As Hydrolytic Media for Cellulose Nanocrystal Production. *Biomacromolecules* 2016, 17, 3025–3032.
- [36] Tri Susanto, Risman Affandy, Gunadi Katon, Rahmani. "Thermal aging properties of natural rubber-styrene butadiene rubber composites filled with modified starch from *Dioscorea Hispida* Denst extract prepared by latex compounding method", AIP Publishing, 2018.
- [37] W T Wulandari, A Rochliadi, I M Arcana. "Nanocellulose prepared by acid hydrolysis of isolated cellulose from sugarcane bagasse", IOP Conference Series: Materials Science and Engineering, 2016.
- [38] Wang, H.; Li, D.; Yano, H.; Abe, K. Preparation of tough cellulose II nanofibers with high thermal stability from wood. *Cellulose* 2014, 21, 1505–1515.
- [39] Wulandari, W T, A Rochliadi, and I M Arcana. "Nanocellulose prepared by acid hydrolysis of isolated cellulose from sugarcane bagasse", IOP Conference Series Materials Science and Engineering, 2016.
- [40] Xu-peng Song, Qiang-hua Wu, Bao-jun Qu. "Photoinitiated crosslinking of EPDM/inorganic filler blends and characterization of related properties", Chinese Journal of Polymer Science, 2009
- [41] Yabin Zhou, Shifeng Wang, Yong Zhang, Yinxi Zhang. " Coated Nano-Sized CaCO Reinforced Semi-Crystalline EPDM ", *Polymers and Polymer Composites*, 2006
- [42] Yanan Zhu, Qincen Yu, Liubin Zheng, Zengyuan Pang, Mingqiao Ge. "Luminous properties of recycling luminous materials SrAlO₃:Eu, Dy based on luminous polyester fabric ", *Materials Research Express*, 2020.
- [43] Yu, H.; Qin, Z.; Liang, B.; Liu, N.; Zhou, Z.; Chen, L. Facile extraction of thermally stable cellulose nanocrystals with a high yield of 93% through hydrochloric acid hydrolysis under hydrothermal conditions. *J. Mater. Chem. A* 2013, 1, 3938–3944.
- [44] Zhang, X.L.; Yang, W.H.; Blasiak, W. Modeling Study of Woody Biomass: Interactions of Cellulose, Hemicellulose, and Lignin. *Energy Fuels* 2011, 25, 4786–4795.
- [45] Zhuo, X.; Liu, C.; Pan, R.T.; Dong, X.Y.; Li, Y.F. Nanocellulose Mechanically Isolated from *Amorpha fruticosa* Linn. *ACS Sustain. Chem. Eng.* 2017, 5, 4414–4420.

Citation: Isha Meshram et al. *Enhancing Mechanical and Thermal Properties of Natural Rubber Composites via Nanocellulose Reinforcement from Coconut Shell Waste: A Sustainable Approach*. *International Journal of Advanced Research in Chemical Science (IJARCS)*. 2024; 11(1):25-36. DOI: <https://doi.org/10.20431/2349-0403.1101003>.

Copyright: © 2024 Authors. This is an open-access article distributed under the terms of the Creative Commons Attribution License, which permits unrestricted use, distribution, and reproduction in any medium, provided the original author and source are credited.